Magnetic resonance hybridization and optical activity of microwaves in a chiral metamaterial

T. Q. Li,[1] H. Liu,[1,a)] T. Li,[1] S. M. Wang,[1] F. M. Wang,[1] R. X. Wu,[2] P. Chen,[2] S. N. Zhu,[1,a)] and X. Zhang[3]
[1]*Department of Physics, National Laboratory of Solid State Microstructures, Nanjing University, Nanjing 210093, People's Republic of China*
[2]*Department of Electronic Sciences and Engineering, Key Laboratory of Modern Acoustics, Nanjing University, Nanjing 210093, People's Republic of China*
[3]*5130 Etcheverry Hall, Nanoscale Science and Engineering Center, University of California, Berkeley, California 94720-1740, USA*

(Received 29 January 2008; accepted 14 March 2008; published online 2 April 2008)

The propagation of microwaves through a chiral metamaterial based on a magnetic dimer is experimentally studied. As proposed by our previous theoretical model, two resonance peaks are obtained in the transmission spectrum; these originate from the hybridization effect of magnetic resonance modes in this system. Optical activity is also observed in the transmission wave. The polarization state dramatically changes around the resonance frequency: the transmitted wave becomes elliptically polarized with its major polarization axis approximately perpendicular to that of the linear incident wave. This coupled magnetic dimer system provides a practical method to optically design tunable active medium and device. © *2008 American Institute of Physics*.
[DOI: 10.1063/1.2905285]

In 1999,[1] Pendry *et al.* reported that a nonmagnetic metallic element—a double split-ring resonator (DSRR)—sized below the diffraction limit exhibits strong magnetic responses and behaves like an effective negative permeability material. Despite the absence of free magnetic poles in such systems, the excitation of displacement currents in the DSRR results in the induction of a magnetic dipole moment that is somewhat similar to a bar magnet. Analogous to the surface plasmon resonance in metal nanoparticles, an effective medium made of DSRRs could support resonant magnetic plasmon (MP) oscillations at gigahertz[1–4] and terahertz frequencies and within the visible spectral region.[4–12] Combined with an electric response and characterized by negative permittivity, such systems could lead to the development of metamaterials with negative indexes of refraction.[2,3]

On the other hand, however, it was also suggested that a combination of magnetic response and chirality could be used as an alternative route to negative refraction.[13] Further, various electromagnetic chiral structures have been reported in the microwave spectral range, such as helical wire spring,[14] swiss-role metal structure,[13] rotating rosette shape,[15,16] and H-shape.[17] In our recent paper,[18] we proposed a theoretical model to show that the coupling effect between two split-ring resonators can be used to produce optical activity and the rotation of polarization can be tuned by changing the coupling strength.

In this paper, we present the first experimental verification of the results proposed by the theoretical model described in Ref. 18. We design and experimentally investigate an array of magnetic dimers (MDs) that are made of two square single split-ring resonators (SSRRs). Further, we focus on the polarization property: an incident wave of linear polarization changes its polarization state when passing through this coupled system. This optical activity is caused by the coupling of the SSRRs and is not observed in the individual SSRR.

Figure 1(a) shows the basic element of the MD and all its characteristic sizes—it comprises two square copper rings with their slits perpendicular to each other—the slit of the first SSRR is parallel to the x axis and that of the second is along the y axis. These two rings are separated by a distance D that is filled with polystyrene (of which the permittivity is 4). Our array comprises these MDs positioned in the x-y plane and the lattice period is set at 4.64 mm.

In the experimental setup [see Fig. 1(b)], a linearly polarized microwave with $\vec{E}$ field along the y direction extends from the source and perpendicularly passes through the plan of our MD array. A detector (Agilent E8363A vector network analyzer) is set on the other side of the plan to receive the transmitted signal; it records the amplitude and phase of both the x and y components of the transmitted wave. Further, the frequency range of the electromagnetic wave is set below 20 GHz based on the measurement capacity of the detector.

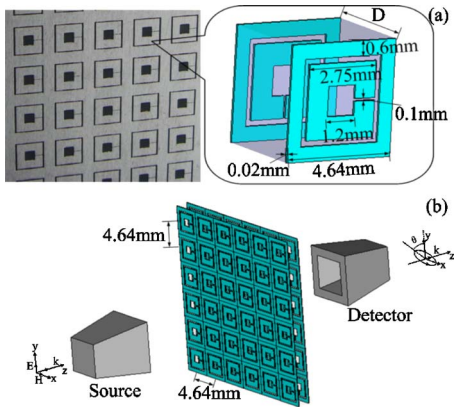

FIG. 1. (Color online) (a) Photograph of magnetic dimers (inset: structure of one unite cell). (b) Schematic picture of the experimental setup, the incident wave is emitted from the source (on the left) and is received by the detector (on the right), the polarization direction of the incident wave is along the y axis.

[a)]Authors to whom correspondence should be addressed. Electronic addresses: liuhuiemail@yahoo.com and zhusn@nju.edu.cn.

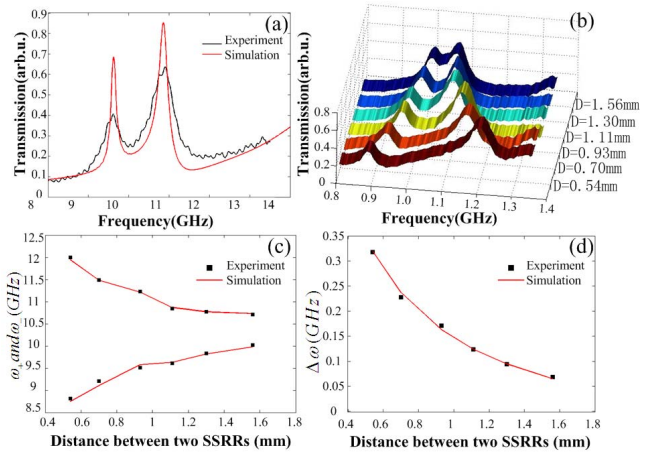

FIG. 2. (Color online) (a) The amplitude of transmitted wave through the array of magnetic dimers with $D=1.11$ mm, experiment result (black line) and simulation result [gray (red) line]. (b) Transmission results under the different D. (c) Resonance frequencies on the distance D. (d) Frequency gap $\Delta\omega=\omega_2-\omega_1$ on the distance D.

Figure 2(a) (black line) shows the experimental result of transmission under $D=1.11$ mm. We observe two obvious resonance peaks in the transmission curve that correspond to the two excited magnetic resonant modes anticipated in our theoretical model.[18] In order to compare and examine the experimental result, we employ finite-difference time-domain simulation by using a commercial software package—CST MICROWAVE STUDIO. The simulated transmission result is also shown in Fig. 2(a) (red line); it is observed that the simulated and experimental results are in good agreement. Then, we tune the thickness of the middle layer between the two SSRRs with six discrete values ranging from 0.54 to 1.56 mm; the measured transmission results for each distance are shown in Fig. 2(b). As the distance D increases, the two resonance peaks gradually join each other with the blurring of their bounds [see Fig. 2(b)], and the frequency gap between the two resonance peaks accordingly decreases [see Figs. 2(c) and 2(d)].

In order to explain the two resonance peaks described above, here, we introduce Lagrangian formalism to describe the MD. We begin from the single SSRR, and then expand it to the coupled condition of our system. One SSRR can be viewed as an ideal LC circuit—the metal ring is regarded as a magnetic loop with inductance L and the slit of the ring is a capacitor with capacitance C. Thus, this system has a resonance frequency of $\omega_0=1/\sqrt{LC}$, and the oscillating current induced in the resonator generates the magnetic moment. If we define the charge accumulated in the slit as a generalized coordinate, the Lagrangian of SSRR can be written in a rather simple form: $\Gamma=L\dot{Q}^2/2-Q^2/2C$. Corresponding, respectively, to the magnetic loop and capacitor, $L\dot{Q}^2/2$ refers to the electrostatic energy stored in the ring, and $Q^2/2C$ refers to the energy in the slit. Accordingly, with an additional interaction term, the Lagrangian of the coupled MD system comprises a combination of the two individual SSRRs:

$$\Gamma = (L/2)(\dot{Q}_1^2 - \omega_0^2 Q_1^2) + (L/2)(\dot{Q}_2^2 - \omega_0^2 Q_2^2) + M\dot{Q}_1\dot{Q}_2.$$

Here, Q_1 and Q_2 are oscillatory charges in the respective SSRRs, M is the mutual inductance, and C is substituted with the relation $\omega_0=1/\sqrt{LC}$.

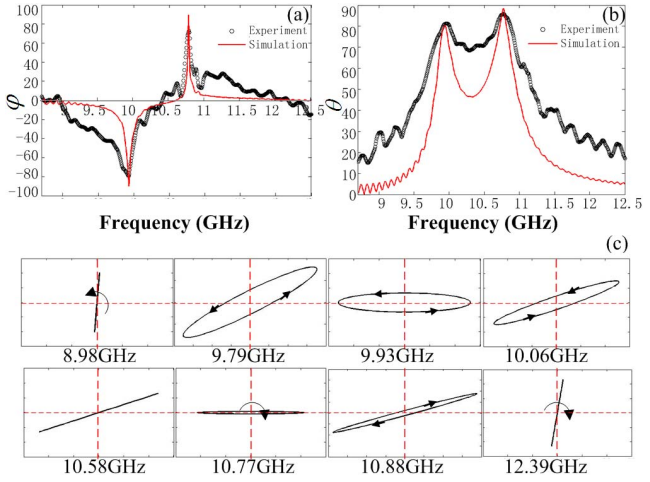

FIG. 3. (Color online) (a) Phase difference φ between x component and y component of transmitted wave: experimental result (black circle) and simulation result [gray (red) line]. (b) Rotation angle of the major polarization axis of transmitted wave (black circle: experiment results; red line: simulated results). (c) The change of polarization state on frequency with $D=1.56$ mm.

By solving the Euler–Lagrange equations, the eigenfrequencies $\omega_\pm=\omega_0/\sqrt{1\mp(M/L)}$ of the MP are obtained. These exhibit two magnetic resonant modes in this coupled system—the antibonding mode $|\omega_+\rangle$ that is characterized by an antisymmetric charge distribution $(Q_1=-Q_2)$, and the bonding mode $|\omega_-\rangle$ that exhibits a symmetric charge distribution $(Q_1=Q_2)$. Further, the frequency split of the two resonant modes $\Delta\omega=\omega_1-\omega_2\approx(M/L)\omega_0$ is changed by the strength of the coupling; thus, as the distance between the two SSRRs increases, the inductance M dramatically decreases, leading to a reduction in the frequency split $\Delta\omega$ [see Figs. 2(c) and 2(d)].

After studying the transmission property, we focus on the optical activity of this periodic array of MDs. For an observer facing the approaching wave, the profile of the E vector can be written as the following well-known equation:[19]

$$\left(\frac{E_x}{|E_x|}\right)^2+\left(\frac{E_y}{|E_y|}\right)^2-\frac{2E_xE_y}{|E_x||E_y|}\cos(\varphi_y-\varphi_x)=\sin^2(\varphi_y-\varphi_x).$$

We define the phase difference between the y and x components as $\varphi=\varphi_y-\varphi_x$. This determines the type of polarization state and the revolving direction: $\varphi=0$ indicates a linearly polarized state, while other conditions denote elliptical or circular polarization. Again, for an observer facing the approaching wave, the end point of the electric field revolves in the clockwise direction when $\sin\varphi>0$ and counterclockwise when $\sin\varphi<0$. We also employ the angle θ, defined as $\theta=\frac{1}{2}\arctan[2|E_x||E_y|\cos\varphi/(|E_x|^2-|E_y|^2)]$,[19] that describes the angle between the major polarization axis and the y axis. This gives us a more intuitive picture about the changing of the elliptical polarization with frequency.

Figure 3 shows the experimental result of φ and θ when we set the distance between the SSRRs as 1.56 mm. From Fig. 3(a), we find that φ becomes zero at a frequency of 10.58 GHz, which divides the phase difference into two parts: negative and positive. Further, around the two resonant frequencies, φ reaches its extrema that are near $-90°$ and $90°$, respectively. At lower frequencies (<10.58 GHz),

$\sin\varphi<0$, the ellipse is counterclockwise, and the dimer constitutes an isomer of *d* type; at higher frequencies (>10.58 GHz), $\sin\varphi>0$, the ellipse becomes clockwise and accordingly, the isomer is *l* type; and at exactly 10.58 GHz, the transmission briefly becomes linearly polarized. The rotation angle of the major polarization axes θ is shown in Fig. 3(b): as the frequency increases, the major polarization axis rotates quickly from the *y* axis and almost reaches the *x* axis at the resonant frequencies. Figure 3(c) presents a more intuitive description of the changing of the polarization state, wherein the curve made by the end point of the *E* vector is shown under eight specific frequencies. In the lower frequency region, the polarization of the transmission is a counterclockwise and compressed ellipse with the major axis slightly off the *y* axis. Then, the ellipse inflates and the major axis rotates toward the *x* axis. With the approach of the first resonant frequency, the ellipse shrinks again and becomes a flat ellipse with a 7° angle between the major axis and the *x* axis at a resonant frequency of 9.93 GHz. When the frequency reaches 10.58 GHz, the transmission becomes linearly polarized, and the ellipse begins to change its rotating direction to clockwise. Then, the ellipse compresses at the second resonant frequency of 10.77 GHz, where we observe that its major axis is almost along the *x* axis (with an angle of 2°). As the frequency increases, the major axis rotates forward to the *y* axis; the ellipse inflates at first but then deflates to a slender one almost horizontal to the *y* axis—similar to that at the low frequency. This indicates that at the resonant frequencies, the *y*-direction polarized incident wave becomes a very prolate elliptical wave with the major polarization axis near the *x* axis when passing through the array of MDs. Further, the area between the two resonance peaks exhibits transitional behaviors: there exist linear and various elliptical polarization states.

As discussed above, the slit of the first SSRR is along the *x* axis so that the incident wave generates a *y*-direction electric field in the slit; thus, this *y*-polarized incident wave is electrically coupled into the system. Through the strong magnetic interaction at the resonant frequency, energy is transferred from the first SSRR to the second one. As the electric field in the second slit is along the *x* axis, the electric dipole radiation generated in this slit gap is *x*-direction polarized. As a result, the transmission is a superposition of the *x*- and *y*-polarized states. At the two resonant frequencies, the interaction becomes extremely distinctive and the *x*-direction polarized wave reaches its maximum value in the transmission; thus, we obtain an elliptically polarized wave with the major axis almost along the *x* direction. Further, in the area far beyond the resonant frequency, a less *x*-direction polarized wave appears in the transmission so that the transmitted wave becomes a compressed ellipse near the *y* axis. As the distance between the SSRRs increases, the frequency gap shrinks and the two elliptical polarization states gradually join.

In this paper, we only realized the optical activity of MDs in the microwave range. Actually, the experimental verification of chiral metamaterials at optical frequencies is more interesting and should be realized in future studies.

In conclusion, we design a MD array comprising two SSRRs and experimentally investigate the behavior of the separated resonance peaks as well as their strong dependence on the distance between the two SSRRs. The optical activity of this periodic array of MDs caused by magnetic interaction is also studied in the transmission measurement; we found that a compressed, elliptically polarized transmitted wave can be achieved at the resonant frequency with the major polarization axes approximately perpendicular to that of the incident wave. Thus, these coupled SSRRs can function as a tunable optical activity medium, and this offers possible applications as a controllable polarizer.

This work was supported by the State Key Program for Basic Research of China (Nos. 2006CB921804 and 2004CB619003), the National Natural Science Foundation of China under Contract Nos. 10534042, 60578034, 10604029, and 10704036, and National Fundamental Fund of Personnel Training (No. J0630316).

[1] J. B. Pendry, A. J. Holden, D. J. Robbins, and W. J. Stewart, IEEE Trans. Microwave Theory Tech. **47**, 2075 (1999).
[2] D. R. Smith, W. J. Padilla, D. C. Vier, S. C. Nemat-Nasser, and S. Schultz, Phys. Rev. Lett. **84**, 4184 (2000).
[3] R. A. Shelby, D. R. Smith, and S. Schultz, Science **292**, 77 (2001).
[4] R. Marqués, J. D. Baena, M. Beruete, F. Falcone, T. Lopetegi, M. Sorolla, F. Martín, and J. Garcia, J. Opt. A, Pure Appl. Opt. **7**, S38 (2005).
[5] T. J. Yen, W. J. Padilla, N. Fang, D. C. Vier, D. R. Smith, J. B. Pendry, D. N. Basov, and X. Zhang, Science **303**, 1494 (2004).
[6] S. Linden, C. Enkrich, M. Wegener, J. F. Zhou, T. Koschny, and C. M. Soukoulis, Science **306**, 1351 (2004).
[7] C. Enkrich, M. Wegener, S. Linden, S. Burger, L. Zschiedrich, F. Schmidt, J. F. Zhou, T. Koschny, and C. M. Soukoulis, Phys. Rev. Lett. **95**, 203901 (2005).
[8] V. M. Shalaev, W. Cai, U. K. Chettiar, H. Yuan, A. K. Sarychev, V. P. Drachev, and A. V. Kildishev, Opt. Lett. **30**, 3356 (2005).
[9] N. Katsarakis, G. Konstantinidis, A. Kostopoulos, R. S. Penciu, T. F. Gundogdu, M. Kafesaki, E. N. Economou, T. Koschny, and C. M. Soukoulis, Opt. Lett. **30**, 1348 (2005).
[10] J. Zhou, Th. Koschny, M. Kafesaki, E. N. Economou, J. B. Pendry, and C. M. Soukoulis, Phys. Rev. Lett. **95**, 223902 (2005).
[11] A. Ishikawa, T. Tanaka, and S. Kawata, Phys. Rev. Lett. **95**, 237401 (2005).
[12] H. Liu, D. A. Genov, D. M. Wu, Y. M. Liu, J. M. Steele, C. Sun, S. N. Zhu, and X. Zhang, Phys. Rev. Lett. **97**, 243902 (2006).
[13] J. B. Pendry, Science **306**, 1353 (2004).
[14] I. Tinoco and M. P. Freeman, J. Phys. Chem. **61**, 1196 (1957).
[15] A. Papakostas, A. Potts, D. M. Bagnall, S. L. Prosvirnin, H. J. Coles, and N. I. Zheludev, Phys. Rev. Lett. **90**, 107404 (2003).
[16] A. V. Rogacheva, V. A. Fedotov, A. S. Schwanecke, and N. I. Zheludev, Phys. Rev. Lett. **97**, 177401 (2006).
[17] J. M. Hao, Y. Yuan, L. X. Ran, T. Jiang, J. A. Kong, C. T. Chan, and L. Zhou, Phys. Rev. Lett. **99**, 063908 (2007).
[18] H. Liu, D. A. Genov, D. M. Wu, Y. M. Liu, Z. W. Liu, C. Sun, S. N. Zhu, and X. Zhang, Phys. Rev. B **76**, 073101 (2007).
[19] J. D. Jackson, *Classical Electrodynamics* (Wiley, New York, 1999).